Pergamon

Int. J. Heat Mass Transfer. Vol. 40, No. 1, pp. 123–129, 1997

0017–9310/97 $15.00 + 0.00

PII: S0017–9310(96)00078–6

Conjugate natural convection heat transfer between two porous media separated by a vertical wall

F. J. HIGUERA
ETS Ingenieros Aeronáuticos, Pza. Cardenal Cisneros 3, 28040 Madrid, Spain

and

I. POP
Faculty of Mathematics, University of Cluj, R-3400 Cluj, CP 253, Romania

(*Received* 28 *March* 1995 *and in final form* 31 *January* 1996)

Abstract—The problem of coupled heat transfer by natural convection between two fluid-saturated porous media at different temperatures separated by a vertical conductive wall is investigated both analytically and numerically, taking account of the two-dimensional thermal conduction in the separating wall. The main parameters of the problem are ε, the ratio of thickness to height of the wall, which is small in our analysis, and α, a measure of the ratio of the thermal resistance of one of the boundary layers to the thermal resistance of the wall. Asymptotic solutions are obtained for large and small values of α and α/ε^2 and compared with numerical solutions obtained for finite values of these parameters. Copyright © 1996 Elsevier Science Ltd.

1. INTRODUCTION

Convective heat transfer in fluid-saturated porous media has received considerable attention over the last thirty years. This interest was stimulated due to the many applications in, for example, chemical catalytic reactors, packed sphere beds, grain storage, thermal insulation engineering, and such geophysical problems as frost heave. Porous media are also of interest in relation to the underground spread of pollutants and to geothermal energy systems. Literature concerning natural convection due to a heated vertical flat plate in a semi-infinite porous medium is abundant. Representative studies in this area may be found in the recent monograph by Nield and Bejan [1]. In these studies, the plate is assumed to be of zero thickness and conduction through it is not accounted for. However, in recent years, in order to better describe the physical reality, there has been a tendency to move away from these idealizations by taking into account the so-called conjugate effects, which arise due to the finite thickness of the plate. In particular, papers by Vynnycky and Kimura [2, 3], Pop *et al.* [4], Pop and Merkin [5], and Lesnic *et al.* [6] have elucidated the effects of the appropriate conjugate parameters on the heat conduction in the solid walls coupled with natural or mixed convection flows adjacent to vertical and horizontal flat surfaces embedded in a fluid-saturated porous medium.

It is worth pointing out that conduction in the walls can have an important effect on the natural convection flows in many practical situations, especially those concerned with the design of thermal insulation; see [7]. To take an example from outside the realm of porous media, heat producing electronic components are often mounted on a printed circuit board (PCB) above a conducting plate. The heat produced is then transferred, both by conduction through the plate to its two ends and by natural convection in the surrounding fluid to the heat sinks. As a result, the heat removing rate from the electronic components will depend on the coupling of the wall conduction and the fluid convection. It is of interest to understand when this coupling is important, since it will directly influence the temperature distribution among the components and thus the design of heat removing mechanisms in practical applications.

Modeling a conjugate heat transfer problem may be complicated because of the strong coupling between the momentum and energy equations in either porous media or Newtonian fluids and the solid walls. Two classes of solutions have appeared in the literature; boundary layer solutions and direct numerical solutions of the complete governing equations. In the first case, longitudinal heat conduction is neglected in both the solid and the fluids, and the resulting parabolic equations are solved numerically using either series expansion methods or finite-difference schemes. Also, an approximate analytical solution exists predicting the average plate temperature and the average Nusselt number for high values of the Rayleigh number [2, 3].

NOMENCLATURE

f_i	reduced stream function of medium i
h	thickness of the plate
k_i	thermal conductivity of medium i
k_w	thermal conductivity of the plate
L	length of the plate
$\overline{Nu}$	overall Nusselt number defined in equation (13)
$\bar{q}_w$	overall heat flux from medium i to the wall, defined in equation (12)
Ra_i	modified Rayleigh number of medium i
$T_{i\infty}$	temperature of medium i far from the plate
x^*, y^*	Cartesian coordinates along and across the plate, respectively.

Greek symbols

α	heat conduction parameter, defined in equation (11)
α_i	equivalent thermal diffusivity of medium i
β	ratio of boundary layer thermal resistances, defined in equation (11)
η_i	non-dimensional variable for medium i
ε	plate aspect ratio
ψ_i^*	stream function for medium i
θ_i	non-dimensional temperature of medium i, defined in equations (9) and (10)
θ_w	non-dimensional temperature of the plate, defined in equation (8).

In contrast, there is comparatively little work on buoyancy induced flows on both sides of a vertical plate of finite thickness separating two semi-infinite fluid-saturated porous media maintained at different temperatures. Bejan and Anderson [8] were the first to present an analytical treatment of this counter-flowing problem using a linearization technique originally described by Ostrach [9] and Gill [10] in the context of buoyancy-induced convection in a viscous fluid. In [8] the contribution of the transversal heat conduction in the plate was considered, but the longitudinal conduction was neglected.

In a very recent paper, Treviño *et al.* [11] presented a thorough theoretical analysis of the conjugate heat transfer across a vertical wall of finite extent separating two fluids at different temperatures, where two counter-flowing natural convection boundary layers develop for large values of the respective Rayleigh numbers. In their analysis, the authors retained the effect of the wall conduction both along and across the plate and established the conditions under which longitudinal conduction and transversal temperature variations are important. Detailed numerical and asymptotic results were presented for the non-dimensional temperature distributions at both surfaces of the plate, the non-dimensional velocity and temperature profiles in both fluids, as well as for the overall Nusselt number.

In this paper we consider the problem analogous to that of Treviño *et al.* [11] for a vertical plate separating two fluid-saturated porous media at different temperatures, which, to the author's knowledge, has not been treated in the past. The present analysis of the problem follows closely that of [11]. Section 2 contains the mathematical formulation of the problem, the numerical and asymptotic solutions are given in Sections 3 and 4, and Section 5 contains a discussion of the results.

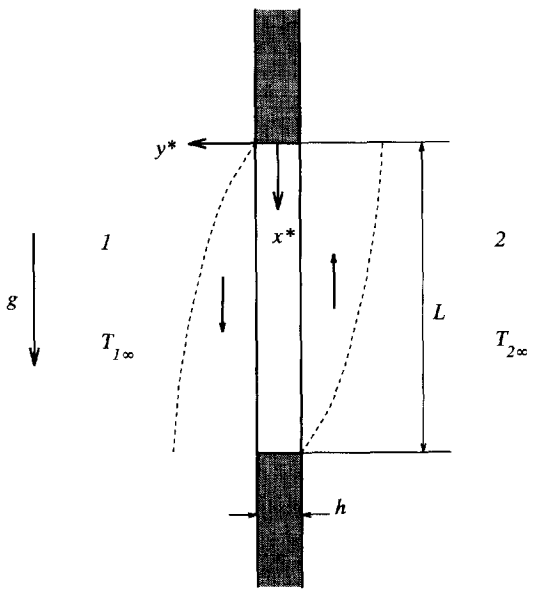

Fig. 1. Physical model and coordinate system.

2. MATHEMATICAL FORMULATION

We consider the two-dimensional configuration presented schematically in Fig. 1. A thin solid vertical flat plate of finite length L and thickness h separates two semi-infinite spaces filled with fluid-saturated porous media at different temperatures. The porous medium at the left-hand side (denoted by the subscript 1) is at a constant temperature $T_{1\infty}$ and the porous medium at the right-hand side (denoted by 2) is at a constant temperature $T_{2\infty}$, where $T_{1\infty} > T_{2\infty}$. We assume that both porous media are isotropic and homogeneous, and that the fluids are incompressible. Invoking the Boussinesq and Darcy approximations, the counter-flowing free convection flows are described by the non-dimensional equations of

momentum and energy for both fluid-saturated porous media

$$\frac{\partial \psi_i}{\partial y_i} = \theta_i \tag{1}$$

$$\frac{\partial \psi_i}{\partial y_i}\frac{\partial \theta_i}{\partial x_i} - \frac{\partial \psi_i}{\partial x_i}\frac{\partial \theta_i}{\partial y_i} = \frac{\partial^2 \theta_i}{\partial y_i^2} \tag{2}$$

where $i = 1, 2$, and the equation of heat transfer inside the solid wall is

$$\frac{\partial^2 \theta_w}{\partial x^2} + \frac{1}{\varepsilon^2}\frac{\partial^2 \theta_w}{\partial y^2} = 0. \tag{3}$$

The boundary conditions for these equations are

$$\left.\begin{aligned} \psi_1 &= 0 \\ \theta_1(x_1, 0) &= 1 - \theta_w(x, 1/2) \\ \frac{\partial \theta_w}{\partial y} &= -\frac{\varepsilon^2}{\alpha}\frac{\partial \theta_1}{\partial y_1} \end{aligned}\right\} \quad \text{at } y_1 = 0 \quad (y = 1/2) \tag{4}$$

$$\left.\begin{aligned} \psi_2 &= 0 \\ \theta_2(x_2, 0) &= \theta_w(1 - x_2, -1/2) \\ \frac{\partial \theta_w}{\partial y} &= -\frac{\varepsilon^2}{\alpha\beta}\frac{\partial \theta_2}{\partial y_2} \end{aligned}\right\} \quad \text{at } y_2 = 0 \quad (y = -1/2) \tag{5}$$

$$\frac{\partial \psi_i}{\partial y_i} = 0 \quad \text{for } y_i \to \infty \tag{6}$$

$$\frac{\partial \theta_w}{\partial x} = 0 \quad \text{at } x = 0, 1. \tag{7}$$

Here the non-dimensional variables are defined as

$$x = \frac{x^*}{L} \quad y = \frac{y^*}{h} \quad \theta_w = \frac{T_w - T_{2\infty}}{\Delta T} \tag{8}$$

for the solid, where x^* is the vertical distance along the wall measured downward from the upper edge, y^* is the horizontal distance from the middle of the wall, T_w is the wall temperature, and $\Delta T = T_{1\infty} - T_{2\infty}$;

$$x_1 = x \quad y_1 = Ra_1^{1/2}\frac{y^* - h/2}{L}$$

$$\psi_1 = \frac{\psi_1^*}{\alpha_1 Ra_1^{1/2}}, \quad \theta_1 = \frac{T_{1\infty} - T_1}{\Delta T} \tag{9}$$

for the downward moving fluid in the boundary layer at the left-hand side of the wall; and

$$x_2 = 1 - x \quad y_2 = -Ra_2^{1/2}\frac{y^* + h/2}{L}$$

$$\psi_2 = \frac{\psi_2^*}{\alpha_2 Ra_2^{1/2}} \quad \theta_2 = \frac{T_2 - T_{2\infty}}{\Delta T} \tag{10}$$

for the upward moving fluid in the boundary layer at the right-hand side of the wall. In the above α_i are the effective thermal diffusivities, ψ_i^* are the stream functions defined in the usual way, and $Ra_i = gK_i\beta_i\Delta TL/\alpha_i\nu_i$ are the Rayleigh numbers for the flows in both porous media, with g being the acceleration due to gravity, and K_i, β_i and ν_i the permeabilities of the media, thermal expansion coefficients and kinematic viscosities of the fluids. In equations (1) and (2) we have tacitly assumed that $Ra_i \gg 1$, i.e. the boundary layer approximation holds.

The non-dimensional parameters, α, β and ε appearing in the problem are

$$\alpha = \frac{k_w}{k_1}\frac{h}{L}\frac{1}{Ra_1^{1/2}} \quad \beta = \frac{k_1}{k_2}\left(\frac{Ra_1}{Ra_2}\right)^{1/2} \quad \varepsilon = \frac{h}{L} \tag{11}$$

with k_i being the thermal conductivities of the porous media and k_w the thermal conductivity of the solid. Here ε is the wall aspect ratio, β is the ratio of the thermal resistances of the two boundary layers, and α is a heat conduction parameter, such that α/ε^2 is the ratio of the thermal resistance of the boundary layer in the hot medium to the thermal resistance of the wall.

The aim of the present work is to determine numerical and asymptotic solutions of the problem (1)–(7) for a range of values of the parameters α, β and ε. These solutions should provide the non-dimensional wall temperature distribution $\theta_w = \theta_w(\alpha, \beta, \varepsilon, x, y)$ and, most importantly, the average heat transfer across the plate

$$\bar{q}_w = \frac{k_1}{L}\int_0^L \left(\frac{\partial T_1}{\partial y^*}\right)_{y^* = h/2} \mathrm{d}x^* = \frac{k_2}{L}\int_0^L \left(\frac{\partial T_2}{\partial y^*}\right)_{y^* = -h/2} \mathrm{d}x^* \tag{12}$$

which can be presented conventionally in terms of the average Nusselt number $\overline{Nu}$ defined as

$$\overline{Nu} = \frac{\bar{q}_w L}{k_1 \Delta T} = -Ra_1^{1/2}\int_0^1 \left(\frac{\partial \theta_1}{\partial y_1}\right)_0 \mathrm{d}x_1. \tag{13}$$

In the following two sections we shall take advantage of the fact that ε is very small in general to classify the solutions according to the values of α and α/ε^2.

3. CASE $\varepsilon \to 0$ WITH $\alpha = O(1)$

In this case the temperature changes across the wall are $O(\varepsilon^2)$ and can be neglected. Laplace's equation (3) can be integrated across the solid giving, upon imposing the boundary conditions (4) and (5) for the heat flux at $y = \pm 1/2$ and using (1) to eliminate the fluid temperatures,

$$\alpha\frac{\mathrm{d}^2\theta_w}{\mathrm{d}x^2} = \left.\frac{\partial^2 \psi_1}{\partial y_1^2}\right|_{y_1 = 0} - \frac{1}{\beta}\left.\frac{\partial^2 \psi_2}{\partial y_2^2}\right|_{y_2 = 0}. \tag{14}$$

The stream functions can be sought in the form

$$\psi_i = x_i^{1/2} f_i(x_i, \eta_i) \quad \text{with } \eta_i = y_i / x_i^{1/2}. \tag{15}$$

Then $\theta_i = f_{i_{\eta_i}}$ and f_i and θ_w are determined by

$$f_{i_{\eta_i\eta_i\eta_i}} + \tfrac{1}{2} f f_{i_{\eta_i\eta_i}} = x_i (f_{i_{\eta_i}} f_{i_{x_i\eta_i}} - f_{i_{\eta_i}} f_{i_{x_i}}) \tag{16}$$

$$\eta_i = 0: \quad f_i = 0, \quad 1 - f_{1_{\eta_2}} = f_{2_{\eta_2}} = \theta_w \tag{17}$$

$$\eta_i \to \infty: \quad f_{i_{\eta_i}} = 0, \tag{18}$$

and

$$\alpha \frac{d^2\theta_w}{dx^2} = \frac{1}{x^{1/2}} f_{1_{\eta_1\eta_1}}\Big|_{\eta_1 = 0} - \frac{1}{\beta(1-x)^{1/2}} f_{2_{\eta_2\eta_2}}\Big|_{\eta_2 = 0} \tag{19}$$

$$\frac{d\theta_w}{dx} = 0 \quad \text{at } x = 0, 1. \tag{20}$$

From (12) and (13), the average Nusselt number is

$$\overline{Nu} = -Ra_1^{1/2} \int_0^1 \frac{\partial^2 f_1}{\partial \eta_1^2}\Big|_{\eta_1 = 0} \frac{dx_1}{x_1^{1/2}}. \tag{21}$$

The problem in equations (16)–(20) was solved numerically using a standard finite-difference method, as described in Treviño *et al.* [11]. Details of the numerical procedure are not presented here as they can be found in [11].

Of interest are also the asymptotic solutions of (16)–(20) for α large and α small, and the subject of the next two subsections is the behavior of the solutions of $\alpha \to \infty$ and $\alpha \to 0$, respectively.

3.1. *Asymptotic limit* $\alpha \to \infty$

For $\alpha \gg 1$ the non-dimensional wall temperature θ_w changes very little in the longitudinal direction, as suggested by the analysis of Treviño *et al.* [11]. In fact this change is of $O(\alpha^{-1})$ as can be seen from equation (19). Therefore, the wall temperature and reduced stream functions can be expressed as power expansions in α^{-1}. Assuming that

$$\theta_w = \theta_{w0}(x) + \alpha^{-1}\theta_{w1}(x) + \cdots \tag{22}$$

equations (19) and (20) lead to $\theta_{w0}(x) = \theta_0 = \text{constant}$, and therefore the flows in the boundary layers are self-similar at this leading order.

A consideration of the boundary conditions (17) suggests looking for a solution of (16) of the form

$$\frac{f_1}{(1-\theta_0)^{1/2}} = \frac{f_2}{\theta_0^{1/2}} = F(\zeta) \tag{23}$$

where

$$\zeta = (1-\theta_0)^{1/2}\eta_1 = \theta_0^{1/2}\eta_2. \tag{24}$$

Substituting (23) and (24) into (19) and integrating the resulting equation over x with the boundary conditions (20) yields

$$\theta_0 = \frac{\beta^{2/3}}{1+\beta^{2/3}}. \tag{25}$$

On the other hand, carrying (23) and (24) into (16)–(18) gives

$$F''' + \tfrac{1}{2} F F'' = 0 \tag{26}$$

$$F(0) = 0 \quad F'(0) = 1 \quad F'(\infty) = 0 \tag{27}$$

where primes denote differentiation with respect to ζ. The solution of this problem is well documented (see Nield and Bejan [1]), and has $F''(0) = 0.444$. Using standard results about the self-similar solution and its invariance under affine transformations, we can obtain the average Nusselt number (21) as

$$\overline{Nu}/Ra_1^{1/2} = 0.888(1-\theta_0)^{3/2}. \tag{28}$$

Expressions (25) and (28) represent the leading order in the expansion of the solution in powers of α^{-1}. We can see that $\theta_{w0} \to 1$ and $\overline{Nu}/Ra_1^{1/2} \to 0$ for large values of β, and $\theta_{w0} \to 0$ and $\overline{Nu}/Ra_1^{1/2} \to 0.888$ for small values of β. The two limits correspond to the cases where the thermal resistance of the very thin boundary layer of fluid 1 or 2, respectively, is negligible and the temperature of the plate is very close to $T_{1\infty}$ or to $T_{2\infty}$. In the particular case in which the porous media at both sides of the wall are the same, $\beta = 1$ and then $\theta_{w0} = 1/2$ and $\overline{Nu}/Ra_1^{1/2} = 0.314$. We notice that (28) can be further improved by computing one more term of the asymptotic expansion (22).

3.2. *Asymptotic limit* $\alpha \to 0$

We can see from the energy equation (14) that the longitudinal heat conduction in the solid becomes negligible for $\alpha \ll 1$ and this equation becomes

$$\frac{\partial^2 \psi_1}{\partial y_1^2}\Big|_{y_1 = 0} = \frac{1}{\beta} \frac{\partial^2 \psi_2}{\partial y_2^2}\Big|_{y_2 = 0}. \tag{29}$$

This relation shows that the heat fluxes from the two porous media are locally equal to each other, and thus both must be finite at the ends of the plate. Then the balance of convection and conduction in (2) implies $[(1-\theta_w), \theta_1] \sim x^{1/3}$ for x small and $(\theta_w, \theta_2) \sim (1-x)^{1/3}$ for $(1-x)$ small, calling for the rescaling

$$\psi_i = x_i^{2/3} \tilde{f}_i(x_i, \tilde{\eta}_i) \quad \text{with } \tilde{\eta}_i = \frac{y_i}{x_i^{1/3}}. \tag{30}$$

In terms of these new variables the problem takes the form

$$\tilde{f}_{i_{\tilde{\eta}_i\tilde{\eta}_i\tilde{\eta}_i}} + \tfrac{2}{3}\tilde{f}_i \tilde{f}_{i_{\tilde{\eta}_i\tilde{\eta}_i}} - \tfrac{1}{3}\tilde{f}_{i_{\tilde{\eta}_i}}^2 = x_i (\tilde{f}_{i_{\tilde{\eta}_i}} \tilde{f}_{i_{x_i\tilde{\eta}_i}} - \tilde{f}_{i_{\tilde{\eta}_i\tilde{\eta}_i}} \tilde{f}_{i_{x_i}}) \tag{31}$$

$$\left.\begin{aligned} \tilde{f}_i &= 0 \\ \tilde{f}_{1_{\tilde{\eta}_1}}(x_1, 0) &= x_1^{2/3} - (1-x_1)^{1/3}\tilde{\theta}_w(x_1) \\ \tilde{f}_{2_{\tilde{\eta}_2}}(x_2, 0) &= x_2^{2/3} - (1-x_2)^{1/3}\tilde{\theta}_w(1-x_2) \\ \tilde{f}_{1_{\tilde{\eta}_1\tilde{\eta}_1}} &= \frac{1}{\beta}\tilde{f}_{2_{\tilde{\eta}_2\tilde{\eta}_2}} \end{aligned}\right\} \quad \text{at } \tilde{\eta}_i = 0 \tag{32}$$

$$\tilde{f}_{i_{\tilde{\eta}_i}} = 0 \quad \text{for } \tilde{\eta}_i \to \infty \tag{33}$$

where

$$\tilde{\theta}_w = \frac{\theta_w + x - 1}{x^{1/3}(1-x)^{1/3}}. \tag{34}$$

4. CASE $\varepsilon \to 0$ WITH $\alpha/\varepsilon^2 = O(1)$

Now the temperature difference between the two faces of the wall is $O(1)$ to fulfil the boundary conditions (4) and (5) for the heat flux at $y = \pm 1/2$. The longitudinal heat conduction is again negligible, except in small regions close to the edges of the wall, and the scaling (30) remains appropriate. Equations (31) and (33) still hold in the fluid-porous media, whereas the boundary conditions (32) at $\tilde{\eta}_i = 0$ become

$$\tilde{f}_i = 0 \tag{35}$$

$$\tilde{f}_{1_{\tilde{\eta}_1}} = \tilde{\theta}_{w_1} \quad \tilde{f}_{2_{\tilde{\eta}_2}} = \tilde{\theta}_{w_2} \tag{36}$$

$$\tilde{f}_{1_{\tilde{\eta}_1\tilde{\eta}_1}} = \frac{1}{\beta}\tilde{f}_{2_{\tilde{\eta}_2\tilde{\eta}_2}} = \frac{\alpha}{\varepsilon^2}[(1-x)^{1/3}\tilde{\theta}_{w_2} - 1 + x^{1/3}\tilde{\theta}_{w_1}] \tag{37}$$

where

$$\tilde{\theta}_{w_1}(x) = \frac{1-\theta_w(x,1/2)}{x^{1/3}} \quad \text{and} \quad \tilde{\theta}_{w_2}(x) = \frac{\theta_w(x,-1/2)}{(1-x)^{1/3}}. \tag{38}$$

The solution of (31), (33) and (35)–(37) determines $\tilde{\theta}_{w_1}$, $\tilde{\theta}_{w_2}$, and the flow in the boundary layers.

We now briefly consider the cases of $\alpha/\varepsilon^2 \gg 1$ and $\alpha/\varepsilon^2 \ll 1$.

4.1. *Asymptotic limit* $\alpha/\varepsilon^2 \to \infty$

When $\alpha/\varepsilon^2 \to \infty$, the heat fluxes in both porous media remain finite and (37) implies $x^{1/3}\tilde{\theta}_{w_1} \to 1-(1-x)^{1/3}\tilde{\theta}_{w_2}$, recovering the limit $\alpha \to 0$ of Section 3.2.

4.2. *Asymptotic limit* $\alpha/\varepsilon^2 \to 0$

When this limit is applied to equation (37), it is readily seen that the heat fluxes in the porous media tend to zero and therefore $\theta_w(x,1/2) \to 1$ and $\theta_w(x,-1/2) \to 0$, except in small regions near the edges of the wall. Following the same procedure of [11], we find that the scaled functions $\tilde{f}_1$ and $\tilde{f}_2$ are of the form

$$\tilde{f}_1 = (\alpha/\varepsilon^2)^{1/3} G(\tilde{\zeta}) \quad \tilde{f}_2 = (\alpha\beta/\varepsilon^2)^{1/3} G(\tilde{\zeta}) \tag{39}$$

where

$$\tilde{\zeta} = (\alpha/\varepsilon^2)^{1/3}\tilde{\eta}_1 = (\alpha\beta/\varepsilon^2)^{1/3}\tilde{\eta}_2. \tag{40}$$

Substitution into (31) gives

$$G''' + \tfrac{2}{3}GG'' - \tfrac{1}{3}G'^2 = 0 \tag{41}$$

with the boundary conditions

$$G(0) = G' + 1 = 0 \quad G'(\infty) = 0 \tag{42}$$

where the primes now denote differentiation with respect to $\tilde{\zeta}$. Equations (41) and (42) describe the flow around a vertical plate with a prescribed heat flux in a porous medium, a problem previously considered by Rees and Pop [12], whose solution has the property $G'(0) = 1.2947$.

The non-dimensional wall temperature θ_w and the overall Nusselt number are

$$\theta_w = y + \frac{1}{2} - \left(\frac{\alpha}{\varepsilon^2}\right)^{2/3} G'(0)\left[x^{1/3}\left(y+\frac{1}{2}\right) + \beta^{2/3}(1-x)^{1/3}\left(y-\frac{1}{2}\right)\right] + \cdots \tag{43}$$

and

$$\frac{\overline{Nu}}{Ra_1^{1/2}} = \frac{\alpha}{\varepsilon^2}\left\{1 - \left(\frac{\alpha}{\varepsilon^2}\right)^{2/3}\frac{3}{4}G'(0)(1+\beta^{2/3}) + \cdots\right\}. \tag{44}$$

It can be readily seen that $\alpha Ra_1^{1/2}/\varepsilon^2 = (k_w/k_1)/\varepsilon$, so that the Nusselt number does not depend on the Rayleigh number to leading order.

5. RESULTS AND DISCUSSION

We first comment the results of the case $\alpha = O(1)$ for $\varepsilon \to 0$. The non-dimensional wall temperature distributions from the numerical solution of (16)–(20) are illustrated in Fig. 2 for different values of α and two values of β. Also included in this figure are the temperature distributions for $\alpha \to 0$, obtained from the solution of (31)–(34), whereas some stream lines and temperature profiles of the hot fluid cor-

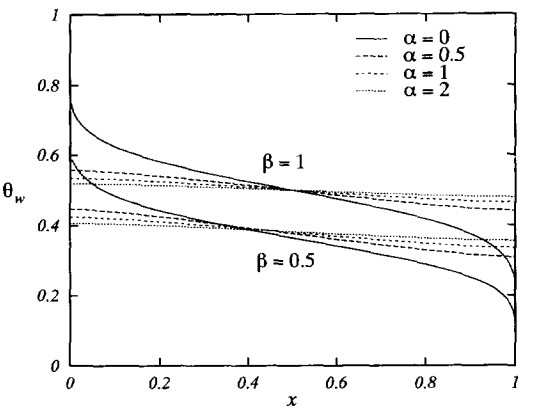

Fig. 2. Non-dimensional wall temperature distribution for several values of α with $\beta = 0.5$ and 1. Results are from the numerical solution.

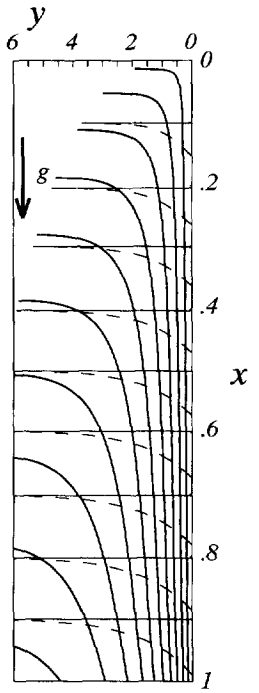

Fig. 3. Streamlines (solid curves) and temperature profiles (dashed) in the boundary layer of the hot medium from the solution for $\alpha \to 0$ with $\beta = 1$. The contour spacing is $\Delta\psi = 0.1$. The streamlines and temperatures in the cold medium are similar to the ones displayed, with the sense of motion reversed.

responding to this limit are displayed in Fig. 3 for $\beta = 1$. In the opposite limit $\alpha \to \infty$ heat conduction along the wall dominates and the wall temperature is uniform, being given by (25) (which yields $\theta_0 = 0.5$ for $\beta = 1$ and $\theta_0 = 0.3865$ for $\beta = 0.5$). As can be seen, longitudinal heat conduction has an important effect even for moderate values of α, rendering the wall temperature distributions almost flat for α greater than about 0.5. We notice that the same trends hold for $\beta = 1$ and for $\beta = 0.5$, but the temperature of the wall increases with β. For very large values of β the problem reduces to that of a uniform wall temperature, equal to the temperature $T_{1\infty}$ of the hot medium at the left of the wall. In the opposite limit of very small values of β the temperature of the wall takes the value $T_{2\infty}$ of the cold medium at the right. The case $\beta = 1$ includes the situation in which the porous media at both sides of the wall are the same.

The solutions for $\beta > 1$ can be easily obtained from those for $\beta < 1$ using the invariance of the problem under the transformation

$$\beta \Rightarrow \frac{1}{\beta} \quad \alpha \Rightarrow \alpha\beta \quad \theta_w \Rightarrow 1 - \theta_w \quad x \Rightarrow 1 - x$$

$$1 \Leftrightarrow 2 \quad \frac{\overline{Nu}}{Ra_1^{1/2}} \Rightarrow \beta \frac{\overline{Nu}}{Ra_1^{1/2}} \tag{45}$$

so only values of $\beta \leqslant 1$ are discussed here.

The overall reduced Nusselt number $\overline{Nu}/Ra_1^{1/2}$ is

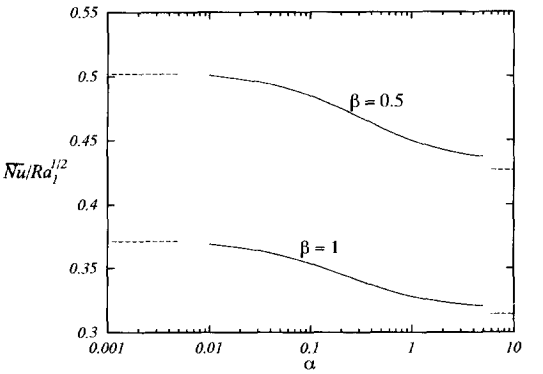

Fig. 4. Overall reduced Nusselt number as a function of α for $\beta = 0.5$ and 1. Results are from the numerical solution (solid curves) and from the asymptotic solutions for small and large values of α.

given in Fig. 4 as a function of α for $\beta = 0.5$ and 1. The asymptotic solutions for large and small values of α (Sections 3.1 and 3.2) are also included here. In essence, the figure illustrates the controlling effect of α, which is seen to be moderate even for very small and very large values of this parameter. This figure also demonstrates that the overall reduced Nusselt number decreases as α increases. As was shown in [11], this is a result to be expected, because increasing α means uniformizing the temperature of the solid and also the temperature difference between the solid and each of the fluids, whereas, owing to the nonlinearity of the boundary layer response, the heat fluxes from the fluids to the solid depend roughly on the temperature differences to the power 3/2, in such a way that the large heat fluxes in regions where the temperature difference is high over-compensate the small fluxes in regions where it is low, rendering the overall heat transfer more efficient for small values of α.

Coming now to the case $\alpha/\varepsilon^2 = O(1)$ for $\varepsilon \to 0$, Fig. 5 represents the variation with x of the non-dimensional temperature θ_w at both faces of the wall for several

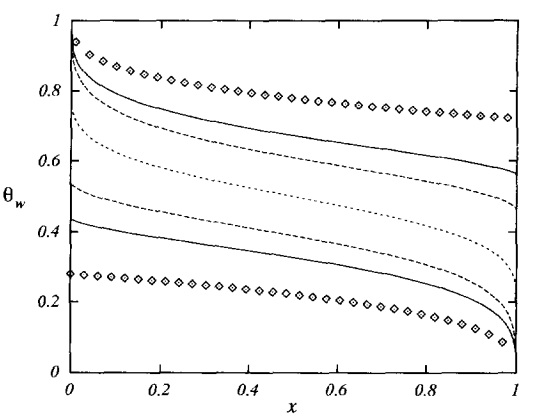

Fig. 5. Non-dimensional temperature distributions at both surfaces of the plate for $\beta = 1$. Results are from the numerical and asymptotic solutions. Upper curves correspond to the side facing the hot medium. Solid: $\alpha/\varepsilon^2 = 0.5$; dashed: $\alpha/\varepsilon^2 = 1$; dotted: $\alpha/\varepsilon^2 \to \infty$; diamonds: asymptotic solution (43) with $\alpha/\varepsilon^2 = 0.1$.

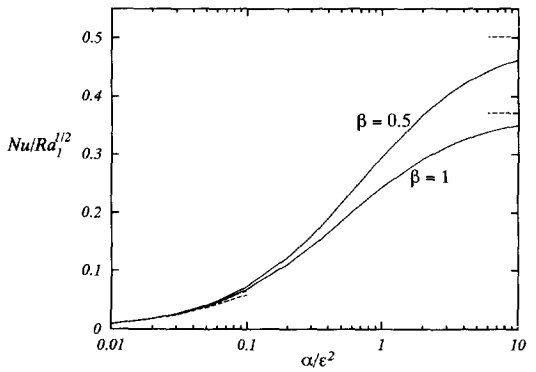

Fig. 6. Overall reduced Nusselt number as a function of α/ε^2 for $\beta = 0.5$ and 1. Results are from the numerical solution (solid curves) and from the asymptotic solutions for small and large values of α/ε^2.

values of the parameter α/ε^2 and $\beta = 1$ (the same porous media at both sides of the wall). Upper curves correspond to the side facing the hot medium and lower curves correspond to the side facing the cold medium. Results from the two-term asymptotic expansion (43) for $\alpha/\varepsilon^2 \ll 1$ are also plotted for $\alpha/\varepsilon^2 = 0.1$ in order to compare with the numerical results. Also, results for the limiting case $\alpha/\varepsilon^2 \gg 1$ are included in this figure. We see that there is a general approach of the numerical results to the asymptotic ones in the corresponding limits.

Figure 6 shows the overall reduced Nusselt number $\overline{Nu}/Ra_1^{1/2}$ as a function of α/ε^2 for two values of β. The numerical results, the two term asymptotic expansion (44) for $\alpha/\varepsilon^2 \ll 1$, and the asymptotic values of $\alpha/\varepsilon^2 \to \infty$ are all three plotted. The agreement between numerical and asymptotic results is excellent for $\alpha/\varepsilon^2 < 0.1$. We see that the overall reduced Nusselt number is an increasing function of α/ε^2, which can be easily explained by noticing that as α/ε^2 increases the temperature difference between the sides of the wall decreases, and thus a larger fraction of the total temperature fall from $T_{1\infty}$ to $T_{2\infty}$ occurs across the boundary layers, leading to larger heat fluxes. From the data in Figs. 4 and 6 we conclude that the overall reduced Nusselt number is maximum for a value of α verifying $\varepsilon^2 \ll \alpha \ll 1$. Indeed, values of this maximum are provided by the solution of the problems (31)–(34) set up in Section 3.2. In Table 1 we give this maximum Nusselt number for several values of β. (Values of $(\overline{Nu}/Ra_1^{1/2})_{max}$ for $\beta > 1$ can be obtained immediately from this table using the transformation (45).)

Table 1.

β	1	0.75	0.5	0.25	0
$(\overline{Nu}/Ra_1^{1/2})_{max}$	0.371	0.421	0.502	0.608	0.888

6. CONCLUSIONS

In this paper we have analyzed the fundamentals of conjugate heat transfer across a vertical flat plate separating two fluid-saturated porous media at different temperatures, where two counter-flowing natural convection boundary layers develop for large values of the respective Rayleigh numbers. In order to gain some insight into the basic heat transfer mechanism, the problem has been solved in the limit of practical interest $\varepsilon \to 0$ for two different cases, namely, $\alpha = O(1)$ and $\alpha/\varepsilon^2 = O(1)$. The nondimensional plate temperature distributions and the overall Nusselt number have been computed as functions of α or α/ε^2, respectively, for different values of β. The limits $\alpha \gg 1$ and $\alpha/\varepsilon^2 \ll 1$ have been also discussed. It has been shown that a maximum overall Nusselt number is obtained for $\varepsilon^2 \ll \alpha \ll 1$. The maximum has been computed as a function of β and the streamlines and temperature distribution of the corresponding flow in the hot medium have been illustrated.

The engineering importance of this study is that it reports means of estimating the heat transfer across a finite vertical wall separating two semi-infinite porous media for cases in which the thermal conductivity of the wall enables heat conduction both across and along it. It is hoped that experimental results will become available in the near future to contrast the results of this theoretical investigation.

REFERENCES

1. D. A. Nields and A. Bejan, *Convection in Porous Media*. Springer, Berlin (1992).
2. M. Vynnycky and S. Kimura, Conjugate free convection due to a vertical plate in a porous medium, *Int. J. Heat Mass Transfer* **37**, 229–236 (1994).
3. M. Vynnycky and S. Kimura, Transient conjugate free convection due to a vertical plate in a porous medium, *Int. J. Heat Mass Transfer* **38**, 219–231 (1995).
4. I. Pop, D. Lesnic and D. B. Ingham, Conjugate mixed convection on a vertical surface in a porous medium, *Int. J. Heat Mass Transfer* **38**, 1517–1525 (1995).
5. I. Pop and J. H. Merkin, Conjugate free convection on a vertical surface in a saturated porous medium, *Fluid Dyn. Res.* **16**, 71–86 (1995).
6. D. Lesnic, D. B. Ingham and I. Pop, Conjugate free convection from a horizontal surface in a porous medium, *J. Appl. Math. Mech. (ZAMM)* **75**, 715–722 (1995).
7. Z.-G. Du and E. Bilgen, Coupling of wall conduction with natural convection in a rectangular enclosure, *Int. J. Heat Mass Transfer* **35**, 1969–1975 (1992).
8. A. Bejan and R. Anderson, Heat transfer across a vertical impermeable partition embedded in a porous medium, *Int. J. Heat Mass Transfer* **24**, 1237–1245 (1981).
9. S. Ostrach, Natural convection in enclosures, *Adv. Heat Transfer* **8**, 161–227 (1972).
10. A. E. Gill, The boundary layer regime for convection in a rectangular cavity, *J. Fluid Mech.* **26**, 515–536 (1966).
11. C. Treviño, F. Méndez and F. J. Higuera, Heat transfer across a vertical wall separating two fluids at different temperatures, *Int. J. Heat Mass Transfer* **39**, 2231–2241 (1995).
12. D. A. S. Rees and I. Pop, Free convection induced by a vertical wavy surface with uniform heat flux in a porous medium, *J. Heat Transfer* **117**, 547–550 (1995).